Progress Towards a Low Power Mixed-Gas Joule-Thomson Cryocooler for Electronic Current Leads

J. M. Pfotenhauer, J. F. Pettitt, D. W. Hoch, and G. F. Nellis

University of Wisconsin - Madison
Madison, WI 53706

ABSTRACT

This paper describes the progress towards a single-stage, low power (< 1 W) mixed gas Joule-Thomson (MGJT) cryocooler for cooling the current leads required by superconducting electronics. By thermally integrating the leads with the recuperative heat exchanger in the MGJT cycle, it is possible to intercept the electrical dissipation and conductive heat leak of the wires at a relatively high temperature thereby providing a thermodynamic advantage. Also, cooling the leads instead of the cryogenic platform may provide some advantages relative to thermal integration.

A model has been developed to optimize the concentration of the MG working fluid and the design of the recuperative heat exchanger. The model incorporates the thermodynamic properties of the mixed gas, accommodates a distributed heat load, includes loss terms for pressure drop, axial conductance, and ineffectiveness, and optimizes the cooling power per conductance ($\dot{Q}$/UA) of the heat exchanger in order to provide the most compact design. For the relatively small amount of cooling power required for the current leads associated with superconducting electronics (~250 mW), the model defines an optimized mixture, appropriate mass flow rates (~ 0.05 g/s) and the necessary heat exchanger conductance, UA (~ 2 W/K).

Two variations of a Hampson type heat exchanger have been designed using the optimization model and constructed to characterize the performance of the MGJT coolers in open and closed cycle operation, and with localized and distributed heat loads. In closed cycle operation, a two-phase, fluid management problem has been identified at very low mass flow rates. The fluid management issue limits the performance of the cooler due to insufficient vapor velocity to prevent excessive liquid accumulation. Operation at higher flow rates has demonstrated the increased performance with a distributed load verses an equivalent load localized at the cold-end.

INTRODUCTION

The mixed gas Joule-Thomson cycle has been identified as an advantageous cooling scheme for current leads because it affords the thermodynamic benefit of absorbing heat over a broad temperature range. Heat is dissipated within a current lead at all points between the room temperature and cryogenic ends, but by integrating the lead with the return-side of the MGJT recuperator, the heat can be absorbed by the refrigerant at all temperatures at which it is generated. The advantage of such a configuration is depicted in Fig. 1. A current lead cooled

Cryocoolers 14, edited by S.D. Miller and R.G. Ross, Jr.

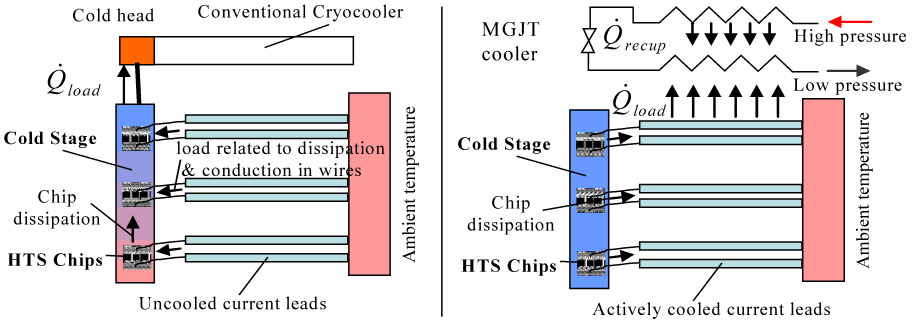

Figure 1. Comparison of heat flow and impact on cold stage of superconducting electronics for uncooled and actively cooled current leads.

with the MGJT system can be converted from a significant heat load on the cold chip platform of the superconducting electronics device where it produces undesirable temperature gradients in the platform, to a localized refrigeration source. An array of such leads then provides the secondary benefit of smoothing out the on-chip temperature profile.

The advantages of mixed gas refrigerants as compared to pure gases in JT coolers have been discussed by many previous authors.[1-4] In addition to the significant cooling power available at relatively low operating pressures, the present application takes advantage of the large temperature range over which two-phase heat transfer enhances the recuperator conductance. A unique characteristic of the present application is that the desired level of cooling power is relatively small (~ 100 mW) and the associated low mass flow rates present challenges for fluid management.

The subsequent section describes the features and use of a model developed to optimize an MGJT cooler that is subjected to a distributed heat load. Details of two different coolers that have been fabricated based on the model are then presented, followed by the performance characteristics of both coolers.

REFRIGERATION SYSTEM MODEL

The model developed for the MGJT cooler presented in this report incorporates multiple unique features. First of all, the model is based on the optimization routine developed by Keppler *et.al.*[5] and utilizes the NIST-4 data-base for gas mixture properties, within a genetic optimization scheme provided by the Engineering Equation Solver (EES) software package[6]. The routine ensures an energy balance for the overall system depicted in Fig. 2 through the following set of equations:

$$h_3 - \frac{\dot{Q}_{rec}}{\dot{m}} = h_5 = h_4 \tag{1}$$

$$h_6 = h_5 + \frac{\dot{Q}_{cold}}{\dot{m}} \tag{2}$$

$$h_1 = h_6 + \frac{\dot{Q}_{rec}}{\dot{m}} + \frac{\dot{Q}_{dist}}{\dot{m}} \tag{3}$$

$$T_1 = T_3 - \Delta T_h \tag{4}$$

$$h_3 = ENTHALPY\left[T_3, P_{high}, gas\ mixture\right]$$
$$h_1 = ENTHALPY\left[T_1, P_{low}, gas\ mixture\right] \tag{5a,b}$$

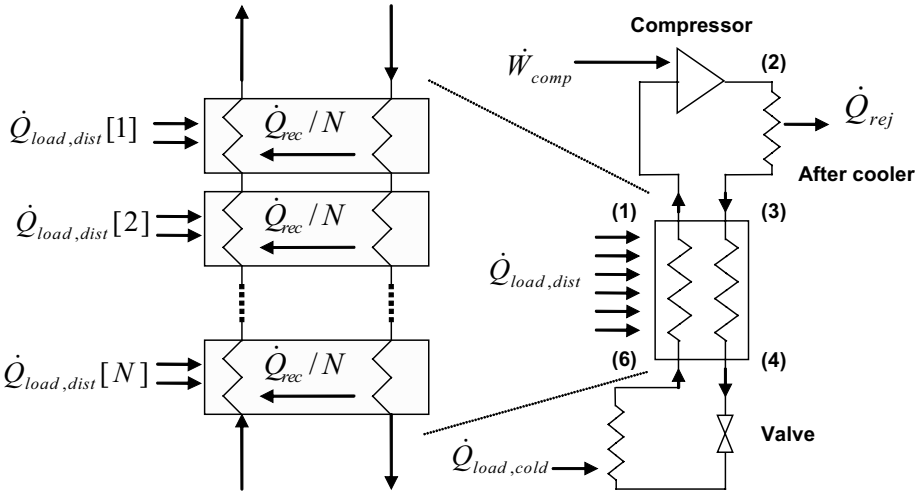

Figure 2. The recuperative heat exchanger broken into N segments of equal recuperative heat transfer.

Here the thermodynamic states around the cooler cycle identified in Fig. 2 are represented by the numbered subscript, while the variables h, T, and P represent the enthalpy, temperature and pressure, respectively. The total heat transferred from the high-pressure flow to the low-pressure flow in the recuperative heat exchanger is represented by $\dot{Q}_{rec}/\dot{m}$ where $\dot{m}$ is the mass flow rate through the system, while the refrigeration per unit of mass flow rate that is absorbed at the cold end and from the distributed load are respectively represented by $\dot{Q}_{load,cold}/\dot{m}$ and $\dot{Q}_{load,dist}/\dot{m}$. As will be shown below, the assumed temperature difference at the warm end of the recuperator, the ratio of distributed to cold-end heat load, and the gas mixture composition provide the variable space over which the system is optimized.

Discretizing

The model further provides a detailed description of the temperature profile within the heat exchanger by discretizing the length into N segments of equal heat transfer per unit mass flow rate $\left[\dot{Q}_{rec}/\dot{m}\right]_i = \dot{Q}_{rec}/\left(N\cdot\dot{m}\right)$. This discretization step is necessary to avoid physically impossible temperature profiles such as a temperature crossing between the high and low pressure streams. For each individual section, fluid properties are assumed constant, and the energy balance for the ith section is defined by the equations

$$h_{high}[i] = h_{high}[i-1] - \frac{\dot{Q}_{rec}}{\dot{m}N} \quad i = 1\ldots N \tag{6}$$

$$h_{low}[i] = h_{low}[i-1] - \frac{\dot{Q}_{rec}}{\dot{m}N} - \frac{\dot{Q}_{load,dist}[i]}{\dot{m}} \quad i = 1\ldots N \tag{7}$$

$$\dot{Q}_{load.dist}[i] = \frac{\dot{Q}_{load,dist}}{N} \tag{8}$$

Here the 1st and the N^{th} sections are at the warm and cold ends of the heat exchanger respectively, while the 'high' and 'low' subscripts respectively refer to the high and low pressure streams. Temperatures at the high and low pressure inlets and exits of each differential section are then obtained from the associated enthalpy and pressure values. For an evenly distributed heat load, one may also define a differential conductance, $dUA[i]$, associated with the ith section

$$\dot{Q}_{load,dist}[i] = \dot{Q}_{load,dist}\frac{dUA[i]}{UA} \tag{9}$$

such that the sum of all the $dUA[i]$ terms equals the total conductance UA. It is possible to model each of the individual heat exchanger segments using conventional ε-NTU type relations in order to estimate the differential conductance required by each segment ($dUA[i]$) and therefore, by integration, the total conductance required by the heat exchanger (UA). However, the conventional ε-NTU type relations that are reported in most text books do not permit a distributed parasitic load and one must therefore use the ε-NTU relationship associated with a counter-flow heat exchanger subjected to a uniform heat flux, (see Nellis and Pfotenhauer[7]).

Optimizing

The procedure described above allows various figures of merit to be computed for the cycle with a specified total conductance; for example, the coefficient of performance (COP) of the cycle (based on a reversible, isothermal compressor model) as well as the refrigeration (the total of the distributed and concentrated loads) per unit of mass flow rate can be computed. However, the most appropriate optimization target for this application is the total refrigeration per unit of heat exchanger conductance ($\dot{Q}/UA$), since maximizing this target provides the most compact refrigeration system. Constraints for the optimization process are defined by the maximum discharge and minimum suction pressures of the compressor, and the warm and cold end temperatures. In addition, the gas mixture must avoid freezing at the cold end. In this regard, the model maintains a 3 degree temperature margin above the freezing point temperature of the mixture (T_{freeze}), the latter being conservatively estimated according to the mole fraction weighted average of the triple points of the various components ($T_{tp,i}$)

$$T_{freeze} = \sum_{i=1}^{NC} y_i \cdot T_{tp,i} \tag{10}$$

where y_i is the mole fraction of component i, and $T_{tp,i}$ is its corresponding triple point temperature.

The optimization results of the model are presented in Fig. 3 as a function of the warm end temperature difference for the constraints used with an APD-HC2 compressor (P_{high} = 1700 kPa,

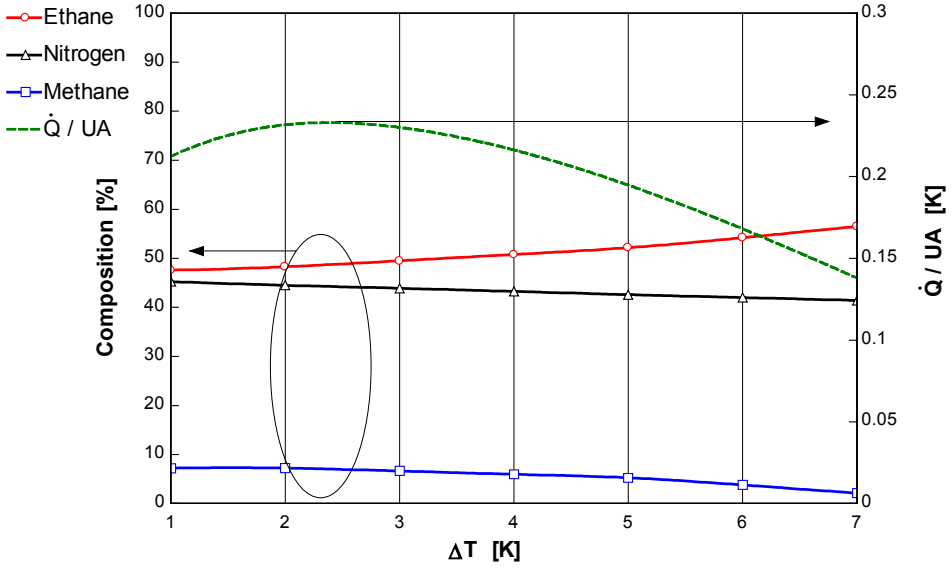

Figure 3. Optimal composition and refrigeration power per unit heat exchanger conductance for $\dot{Q}_{load,dist} / \dot{Q}_{load,cold} = 1$.

P_{low} = 100 kPa), with the warm and cold temperatures of 300 K and 85 K respectively, and for a 3-component mixture of methane, ethane and nitrogen. Notice that the optimal composition with respect to the variable ΔT occurs at a hot end temperature difference (which for this mixture is equivalent to the pinch point temperature difference) between 2 and 3 K. Although a perfect recuperator provides the maximum refrigeration as ΔT approaches 0 K, systems with a small ΔT require a larger heat exchanger (as ΔT approaches zero, the required conductance becomes infinite). Above some value of conductance (i.e., below some value of ΔT) there is a diminishing incentive (in terms of $\dot{Q}/UA$) to bring the temperatures of the streams closer together.

Loss terms

The discussion to this point has described the thermodynamic considerations inherent in the model. In order to include fluid dynamic and heat transfer effects, it is necessary to select a heat exchanger geometry. In this project, a Hampson style heat exchanger is chosen, and the losses associated with pressure drop, flow-dependent heat exchanger ineffectiveness, and axial conduction are determined. Figure 4 presents the geometry of a generic Hampson style heat exchanger. The high pressure (hot) stream flows through the inside of the finned tube, while the low pressure (cold) stream flows past the finned tube.

Flow through both the high and low pressure sides of the heat exchanger includes regions of single phase and two-phase flow. The pressure drop in each region is calculated via correlations that account for the helical flow path, the presence (or not) of fins, and the single or two-phase flow state. Details regarding these calculations are presented in the recent thesis of one of the authors[8]. In practice, it is found that the pressure drop through the inside of the finned tube can be significant and contributes a notable loss to the system performance, but the pressure drop on the finned side of the heat exchanger is negligible.

The differential conductance $dUA[i]$ for the Hampson style heat exchanger may be calculated from the thermal resistance to heat flow between the hot and cold fluid:

$$\frac{1}{dUA[i]} = \frac{1}{htc_h[i]A_h[i]} + \frac{\ln\left(r_{ft,o}/r_{ft,i}\right)}{2\pi k_f dL} + \frac{1}{\eta_o[i]\, htc_c[i]\; A_t[i]}. \tag{11}$$

Here htc_h and htc_c are the convective heat transfer coefficients on the hot and cold sides, respectively, of the finned tube, and A_h and A_t are the surface areas transferring heat from the hot to the cold streams respectively. The subscript 't' on the cold side reflects the fact that the

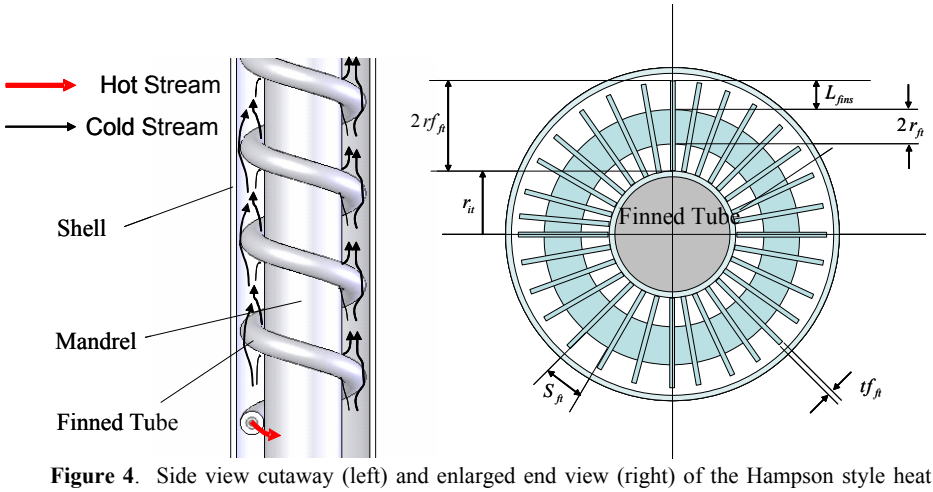

Figure 4. Side view cutaway (left) and enlarged end view (right) of the Hampson style heat exchanger. For clarity, the fins are not included in the side view. Finned tube geometry defined by r_{it}, inner tube (mandrel) radius; tf, fin thickness; r_{ft}, outer radius of finned tube; rf, fin outer radius; S_{ft}, fin spacing; and $L_{fin} = rf - r_{ft}$, the 'length' of the fin.

surface area involved on the cold side is the total, or combined, surface area of the finned and non-finned area of the tube. The terms $r_{ft,o}$, $r_{ft,I}$, $k_{ft,}$ and dL represent respectively the outer and inner radius of the (bare) finned tube, its thermal conductivity, and the differential length associated with the differential conductance $dUA[i]$. η_o is the overall efficiency of the fin array. Although recent measurements[9] provide estimates of the heat transfer coefficients for two-phase mixed gas flow, the model can also use correlations associated with single-phase flow, thus providing a conservative calculation of the differential conductance. For details regarding the specific correlations and length scales involved, the reader is again referred to the recent thesis[8].

Thermal conduction along the axis of the Hampson heat exchanger is calculated from Fourier's law and the various lengths, cross sectional areas, and temperature dependent thermal conductivities associated with the inner tube (mandrel), the outer tube (low pressure enclosure), and the finned tube.

HEAT EXCHANGER CONSTRUCTION AND TESTING

Two different Hampson style heat exchangers have been designed and constructed based on the model described above. The geometries of the two designs are defined in Table 1. Note that the primary difference between the two designs is the number of parallel flow paths provided on the high pressure side of the heat exchanger. Design A incorporates a single finned tube wound on a 0.315 m long mandrel, while design B utilizes three tubes co-wound on the same length of mandrel.

Performance predictions from the model for the two designs are shown in Figures 5a and 5b, for the case where the ratio of distributed to cold end heat load is unity. At the lowest values of mass flow, the capacity of the cooler approaches that of the ideal heat exchanger case where the cooling power increases linearly with the mass flow rate. At the higher mass flow rates, the heat

Table 1. Geometric Parameters for Hampson style heat exchangers.

	mandrel		shell		finned tube		
design	OD	wall thickness	ID	wall thickness	tube inner radius	tube outer radius	fin outer radius
	(mm)	(mm)	(mm)	(mm)	(mm)	(mm)	(mm)
A	3.40	0.203	5.842	0.254	0.140	0.267	0.520
B	12.32	0.203	18.59	0.254	0.521	0.737	1.499

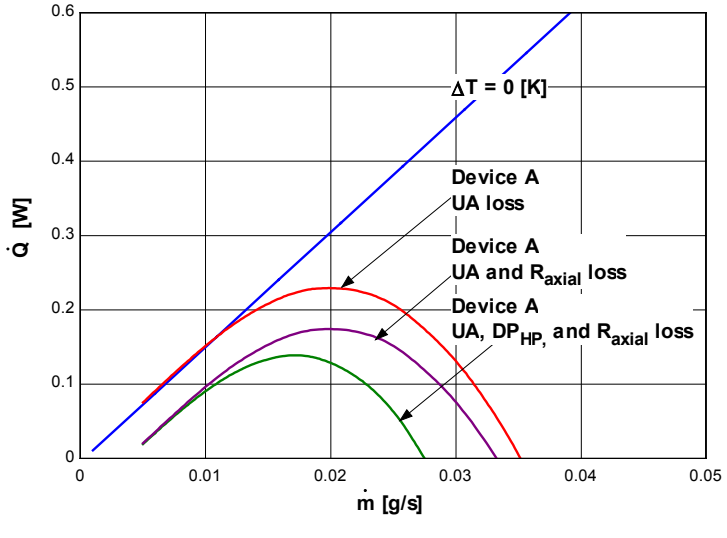

Figure 5a. Model predicted cooling power for device A.

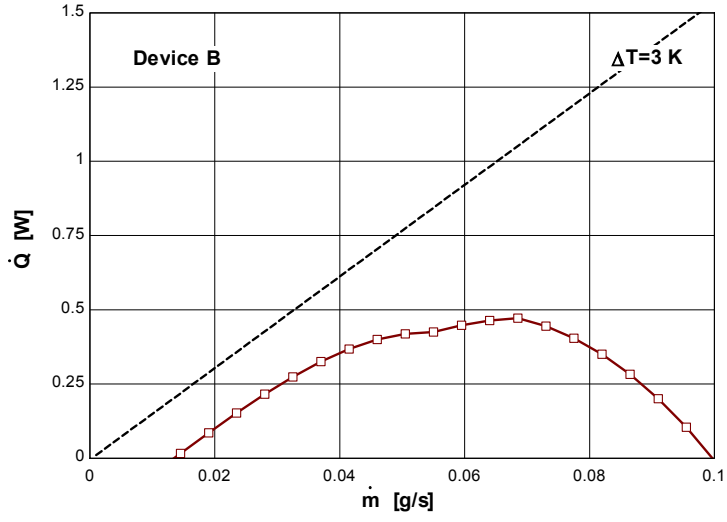

Figure 5b. Model predicted cooling power for device B.

exchanger behaves as expected from *NTU*-ε considerations, in that the effectiveness decreases with increased mass flow rate. Equivalently the warm end temperature difference grows as the mass flow rate increases. Figure 5a explicitly displays the relative influence of each of the loss mechanisms on the predicted cooler performance for design A. The lowest curve indicates the predicted performance, whereas the higher curves are associated with one or more loss terms being "turned off" in the model. The optimum mass flow rates of 0.018 g/s and 0.06 g/s for designs A and B provide respective cooling capacities of 130 mW and 500 mW, both of which are appropriate for the superconducting electronics application.

Testing

Heat exchangers fabricated according to design A and design B have been tested in the facility displayed in Fig. 6. Gas handling equipment (not shown) is used to produce a variety of both pure and mixed gas fluids circulated to and from the MGJT cooler by an APD-HC2 compressor. Fixed size orifices are mounted at the cold end of the recuperator, while the mass flow rate, pressures, and temperatures are monitored through the duration of each test run. A liquid nitrogen cold trap is also included in the gas circulation system to eliminate contaminants that might otherwise block the orifice and halt the gas flow. Prior to utilizing the Hampson style heat exchangers, a simple tube-in-tube heat exchanger was used along with energy balance calculations to measure the parasitic heat load on the recuperator and to verify operation of all the instrumentation. A liquid-nitrogen jacketed dewar is used to reduce the parasitic heat load.

Fixed orifice sizes of 0.0632 mm and 0.152 mm are used with device A to produce flow rates near the optimum value displayed in Fig. 5a. However, it is observed that the system is unable to maintain a non-zero flow rate indefinitely for either the optimized mixture identified in Fig.3 or for pure ethane or pure methane flows. By using a combination of the pressure and temperature measurements near the orifice and the T-S diagrams for pure ethane or methane, it is confirmed that the low flow rates targeted with device A have insufficient inertia to circulate the liquid forming on both sides of the orifice. Rather, as the liquid fraction accumulates first on the high pressure side, and then on the low pressure side of the orifice, the overall flow decreases, eventually ceasing altogether. An example of such behavior is also demonstrated in Fig. 7 for a mixture of 71% nitrogen and 29% ethane. Note that the flow rate ($\dot{V}$) begins decreasing near 57,000 seconds and eventually diminishes to zero. The severity of the problem can be appreciated by noting that the quality of the mixture at the hot outlet and cold inlet ports is no

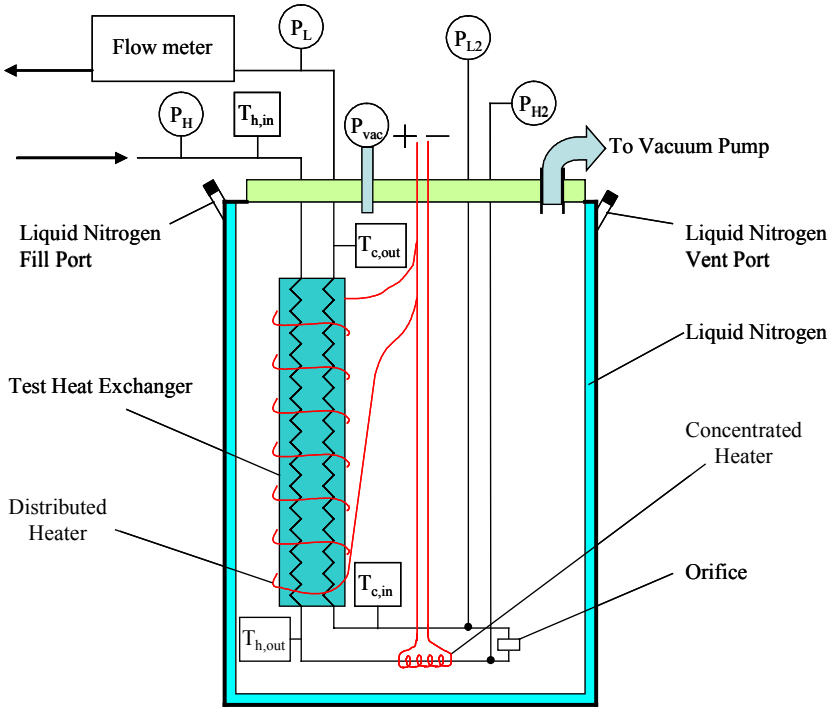

Figure 6. Test facility for mixed gas J-T systems. Measurements provided for high pressure (P_h), low pressure (P_L), hot temperature (T_h) and cold temperature (T_c).

less than 95 % for all the data from 60,000 to 80,000 seconds. The tolerance for the formation of liquid at the orifice is quite low.

The performance of device B with the three parallel high pressure flow paths avoids the flow management problems of device A when an orifice 0.304 mm diameter is used. A similar flow management problem does occur when the 0.152 mm diameter orifice is used. The cooling

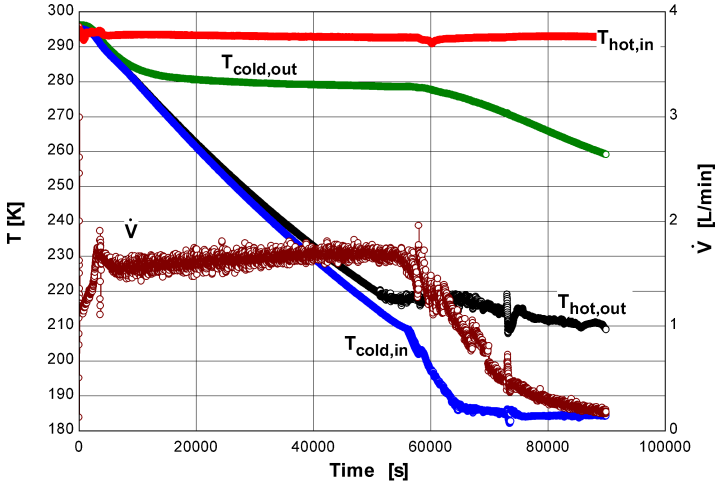

Figure 7. Temperatures and flow rates in device A with a mixture of 71% nitrogen, 29% ethane.

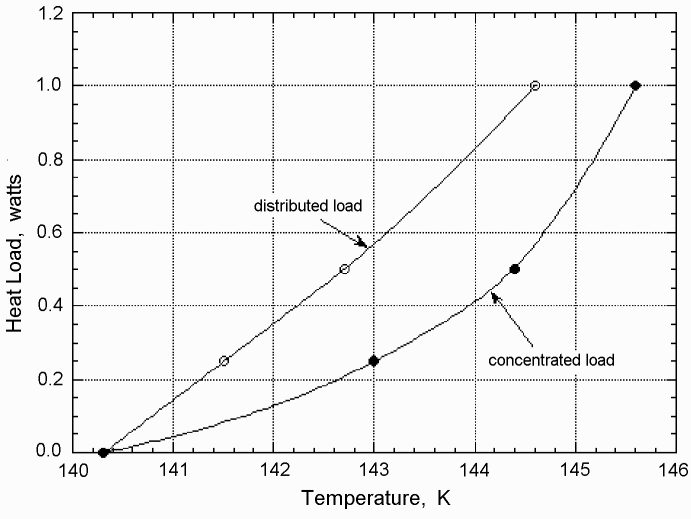

Figure 8. Measured cooling power of device B using a 0.304 mm diameter orifice.

power of device B with the larger orifice is characterized in Fig. 8 with a mixture of 39% nitrogen, 55% ethane, and 6% methane with both a concentrated heat load (all at the cold end) and a purely distributed heat load (no heating at the cold end). As expected, the cooling capacity in the distributed case is larger. As evidenced in Fig. 8, the cooling capacity is increased by more than a factor of 2 for the distributed load as compared to the concentrated load. The fluid management problem identified above has limited the performance of the device. To date, the coldest temperature recorded with either device A or B in closed cycle operation is 110 K, while temperatures less than 88 K can be achieved in open cycle operation.

SUMMARY

A comprehensive model has been developed to optimize the design of mixed gas Joule-Thomson coolers. The model incorporates fluid properties from NIST-4 for gas mixtures, accommodates distributed heat loads, provides temperature profiles through the entire recuperative component of the MGJT system, and enables optimization for a variety of target parameters. Use of the model with Hampson style heat exchangers has been demonstrated for optimizing the heat load per conductance of the heat exchanger, thereby minimizing the size of the recuperator. Two heat exchangers designed by the model have been tested with pure and mixed gases and with concentrated and distributed heat loads. A flow management problem is identified when the mass flow rates have insufficient inertia to entrain the liquid that forms on both sides of the orifice.

ACKNOWLEDGMENT

This work was supported by the Office of Naval Research under grant # N00014-03-1-0175.

REFERENCES

1. Alfeev, V. N., et al., Great Britain Patent, No. 1,336,892, (1973).
2. Longsworth, R.C., Boiarski, M.J., and Klusmier, L.A., "Closed Cycle Throttle Refrigerator," *Cryocoolers 8*, Plenum, New York (1995), pp. 537-541.

3. Alexeev, A., Haberstroh, Ch., Quack, H., "Further Development of a Mixed Gas Joule Thomson Refrigerator", *Advances in Cryogenic Engineering,* Vol 43, (1997), pp. 1667-1674.

4. Boiarski, M., et al., "Design Optimization of the Throttle-Cycle Cooler with Mixed Refrigerant", *Cryocoolers 10*, Kluwer Academic, New York, (1998), pp. 457-465.

5. Keppler, F., Nellis, G., and Klein, S., "Optimization of the Composition of a Gas Mixture in a Joule-Thomson Cycle", *International Journal of Heating, Ventilation, Air Conditioning, and Refrigeration Research*, Vol 10, No. 2, April (2004), pp. 213-230.

6. Klein, S.A., EES – *Engineering Equation Solver*, F-chart Software (2005).

7. Nellis, G.F., and Pfotenhauer, J.M., "Effectiveness-Ntu relationship for a counterflow heat exchanger subjected to an external heat transfer," *Journal of Heat Transfer*, vol. 127, No. 9, (2005), pp. 1071 – 1073.

8. Pettitt, J.F., "Numerical Modeling and Experimental Testing of a Mixed Gas Joule-Thomson Cryocooler," M.S. thesis, Department of Mechanical Engineering, University of Wisconsin-Madison, (2006).

9. Nellis, G.F., Hughes, C.B., and Pfotenhauer, J.M., "Heat Transfer Coefficient Measurements for Mixed Gas Working Fluids at Cryogenic Temperatures," *Cryogenics*, Vol. 45, No. 8, August, (2005), pp. 546-556.